Determination of the Asphaltene Precipitation Envelope and Bubble Point Pressure for a Mexican Crude Oil by Scanning Transitiometry

ARTICLE *in* ENERGY & FUELS · MARCH 2013

Impact Factor: 2.79 · DOI: 10.1021/ef301449e

5 AUTHORS, INCLUDING:

Aquino Olivos Marco Antonio
Instituto Mexicano del Petroleo
17 PUBLICATIONS **68** CITATIONS
SEE PROFILE

Jean-Pierre E Grolier
Université Blaise Pascal - Clermont-Ferrand II
257 PUBLICATIONS **4,099** CITATIONS
SEE PROFILE

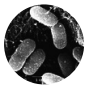

Adriana de J. Aguirre-Gutierrez
Instituto Mexicano del Petroleo
4 PUBLICATIONS **8** CITATIONS
SEE PROFILE

energy&fuels

Article

pubs.acs.org/EF

Determination of the Asphaltene Precipitation Envelope and Bubble Point Pressure for a Mexican Crude Oil by Scanning Transitiometry

Marco A. Aquino-Olivos,*[,†] Jean-Pierre E. Grolier,[‡] Stanislaw L. Randzio,[§] Adriana J. Aguirre-Gutiérrez,[†] and Fernando García-Sánchez[∥]

[†]Programa de Aseguramiento de la Producción de Hidrocarburos, Instituto Mexicano del Petróleo, Eje Central Lázaro Cárdenas 152, 07730 México, D.F., México

[‡]Laboratoire de Thermodynamique des Solutions et des Polimères, UMR CNRS 6003, Université Blaise-Pascal, 24 Avenue des Landais, 63177 Aubière, France

[§]Institute of Physical Chemistry, Polish Academy of Sciences, ul. Kasprzaka 44/52, 01-224 Warszawa, Poland

[∥]Laboratorio de Termodinámica, Programa de Investigación en Ingeniería Molecular, Instituto Mexicano del Petróleo, Eje Central Lázaro Cárdenas 152, 07730 México, D.F., México

ABSTRACT: In this work, the phase transitions (liquid−solid, liquid−vapor, and solid−liquid) for a Mexican crude oil were measured with the transitiometric technique over wide temperature and pressure ranges to determine its asphaltene envelope. A titration of this crude oil with *n*-heptane based on ASTM D3279 and ASTM D4124 standard methods was carried out to make sure that the phase transition corresponds to the asphaltene precipitation. As a result of the experimental work performed here, it is shown that scanning transitiometry is a suitable experimental technique that can be used to determine the asphaltene precipitation onset and the bubble point pressures for a variety of crude oils, where the density of the crude oil is not a limiting factor. The thermodynamic modeling of the asphaltene precipitation envelope was successfully performed using the statistical associating fluid theory for potentials of variable range (SAFT-VR) equation of state (EoS) in the framework of the McMillan−Mayer theory, as reported by Buenrostro-Gonzalez et al. (*AIChE J.* **2004**, *50*, 2552−2570). A satisfactory representation of the bubble pressures line was obtained using the Peng−Robinson (PR) EoS.

INTRODUCTION

Planning and optimization of hydrocarbon production depend, to a large extent, upon the type of hydrocarbons to process. An important aspect in the optimization of the production is the phenomenon of phase changes that occur in hydrocarbon mixtures. In this context, precipitation of asphaltenes and waxes is some of the main problems that affect the crude oil production.[1,2] The formation of deposits of asphaltenic type can take place at the reservoir, in the well, in the pipes, or in the production facilities, while the precipitation of waxes happens when an abrupt change occurs in the temperature but can also occur at the same places where the asphaltenes are deposited.

This kind of phenomena seriously affects the production operations and generates an increase in the production costs because of the treatments required to avoid the precipitation and remediation of the formed deposits. However, although the precipitation of asphaltene is a well-known problem and the main object of numerous investigations in the oil industry, the precipitation of waxes occurs, generally, over the temperature range from 233 to 341 K.[3]

In general, asphaltenes are polydisperse mixtures of different aromatic molecules with alkyl groups and high polarity because of the presence of heteroatoms (N, O, and S) and metals (Ni, V, and Fe).[4] An abrupt change along the production line of the crude oil can cause the asphaltene precipitation. The asphaltenes that are present in the crude oil of the production fields are defined as the matter that precipitates from this oil because of depressurization.

Asphaltenes are present in the crude oil from 0 to 56% (w/w), and they have a drastic effect on the physical and chemical properties of the crude oil. These compounds have molecular weights ranging from hundreds to thousands of atomic mass units, depending upon the origin of the oil. They consist of an aromatic system with 4−10 fused aromatic rings, with compounds substituted peripherally. The asphaltene precipitation, induced by a pressure reduction, is a continuous process, which starts with the first appearance of the asphaltene flocculation.[1]

Asphaltenes and resins are associated in crude oils and generate the aggregation phenomenon as well as flocculation. Mono- and polydisperse asphaltenes are part of the heavy fraction mixture, and both are responsible for the complex behavior observed in the crude oil.[1]

To design and optimize the production lines and improve the flow performance, it is essential to ascertain the conditions of pressure, temperature, and composition at which the aggregation of the organic matter begins and to determine the formation and dissolution enthalpies of the organic aggregates, which triggers off the oil precipitation of the organic matter as well as its redisolution.

In Mexican oil fields, the precipitation and organic matter deposition (asphaltenes and waxes) are a main concern that

Received: September 13, 2012
Revised: February 6, 2013
Published: March 5, 2013

   dx.doi.org/10.1021/ef301449e | *Energy Fuels* 2013, 27, 1212−1222

cause obstruction problems and, hence, deferred production, hydrocarbon production that is delayed as a result of any of several reasons (well repairs, restrictions that diminish production, regulations, etc.).[5] This provokes an increase in the production costs for unplugging and cleaning the production pipes. This is a crucial aspect, because oil reservoirs containing heavier crude oils are presently being exploited [American Petroleum Institute (API) gravity of <22°] in Mexico (and other countries in the world), which represents a severe problem for the recovery of heavy hydrocarbons.

In addition, the plugging can also result from organic matter condensation because of a difference of temperature in the seabed during the production of the crude oil in offshore locations. This implies the necessity of using an appropriate methodology for maintaining the flow performance, taking into account the pressure and temperature profiles with regard to the precipitation envelope of organic matter for each well.

To implement a new methodology that would help to understand some of the problems on flow performance without caring about the type of crude oil to treat, the transitiometric technique was applied to determine the precipitation envelope of the organic matter (asphaltenes) for a crude oil under different conditions of temperature and pressure. This envelope could be established along pressure and temperature profiles, to determine the pressure interval at which the organic matter precipitation phenomenon can be observed. The application of this technique would also be useful for understanding the agglomeration process of the aggregate from the kinetics point of view. The transitiometric technique is also appropriate to investigate the reproducibility of a possible reversible phenomenon induced by temperature, pressure, or volume change.[6]

In this work, the transitiometric technique was used to determine the asphaltene precipitation envelope (APE) and bubble point pressure line for a Mexican crude oil. The thermodynamic modeling of the APE was performed using the statistical associating theory for potentials of variable range (SAFT-VR) equation of state (EoS) in the framework of the McMillan−Mayer theory, as reported by Buenrostro-Gonzalez et al.[7]

EXPERIMENTAL SECTION

Materials. *n*-Heptane was acquired from Aldrich with a 99.9% mol purity and was used without any further purification. A Mexican crude oil (A-1) sample provided by the Mexican Petroleum Institute was used in this work. The principal properties of this crude oil sample are given in Table 1.

Apparatus. The scanning transitometer used in this study to determine the APE for a crude oil over the temperature range from 344 to 427 K and pressures up to 100 MPa is presented in Figure 1.

Table 1. Crude Oil Fluid (A-1) Characterization

property	crude oil sample
saturates (wt %)	60.5
aromatics (wt %)	32.7
resins (wt %)	6.3
asphaltenes (wt %)	0.5
GOR (m^3/m^3)	220.8
density (g/cm^3)	0.68
molecular weight (g/mol)	258.5
reservoir temperature (K)	427.0
reservoir pressure (MPa)	29.7

Notwithstanding, this apparatus can be employed for measuring bubble point pressures of fluids over a wide range of temperatures from 253 to 673 K and pressures up to 400 MPa. This apparatus, with some minor arrangements of the pressure line, was also used for the crude oil titration measurements.

A detailed description of the scanning transitiometer is given elsewhere,[8,9] including some applications of the transitiometric technique,[6,10−13] with only a brief description of the apparatus being presented here. In this apparatus, two vessels, the measuring cell containing the sample under study and the reference cell serving only as a thermal reference,[14] are placed in a differential mounting inside the calorimetric block detector, with itself being thermally insulated. The calorimetric vessels are made of stainless-steel 316 cylinders with an internal diameter of 7.9 mm, withstanding a maximum pressure of 200 MPa.

The sample under investigation is loaded[15,16] inside the calorimetric vessel, which is connected to the temperature, pressure, and volume sensors. The displacement of the pressurizing fluid (Hg in this case) into the system is carried out using a positive displacement pump with a total displacement volume of 9 mL, with each step of the pump stepping motor corresponding to a calibrated displacement volume of $(5.24 \pm 0.04) \times 10^{-6}$ mL.

The calibration of pressure detectors 1 and 2 shown in Figure 1 (Viatran 245) was verified with a dead-weight gauge over a pressure range from 0.1 to 400 MPa. Pressure measurement uncertainties are estimated to be 0.15% of the pressure full scale. The temperature indicator was calibrated against a Pt resistance thermometer placed inside the high-pressure calorimetric vessel. Temperature measurement uncertainties are estimated to be ±0.1 K. The energy scales were calibrated using a reference material (a primary standard). The temperature measurements both absolute and differential were monitored with a calibrated platinum resistance thermometer with a 100Ω sensor.[11]

The pressure sensors, the stepping motor, the temperature controller, and the calorimetric amplifier are connected to a digital control module. The software elaborated with Virtual Instrument (VI) LabView language allows for independent control and recording of the pressure p, temperature T, and volume V through the control of the pump steps (see Figure 1). These variables can be scanned simultaneously during all of the experimental processes.[8,9]

Scanning Transitiometry. The principle of the scanning transitiometric technique is shown schematically in Figure 2. In this experimental technique, a transitiometer with two calorimetric vessels is used for monitoring the pressure p, the temperature T, and the volume V, as well as the time t and the calorimetric signal. From the variation of the dependent variables and the effects of the associated heat, the thermodynamic coefficients and the change of the phases under study are determined accurately. The scanning rate of either temperature or pressure allows for monitoring of the thermodynamic behavior of the system enclosed in the transitiometric vessel. Therefore, it is possible to carry out a complete thermodynamic study for an extended $p-V-T$ surface over wide ranges of temperature and pressure, which allows for asphaltene reversibility (asphaltene re-incorporation in crude oil), if it exists, of the phase transitions. The reversibility of the asphaltene precipitation/flocculation process is a subject of some controversy in the literature. Some researchers believe that asphaltene precipitation is not reversible. This conclusion is based on certain experimental observations of the colloidal behavior of asphaltene suspensions.[17,21] Flotland[18,21] and Wang et al.[19,21] have speculated that asphaltene precipitation is less likely to be reversible for crude oils subjected to conditions well beyond those of the precipitation onset. Hirschberg et al.[20,21] have assumed that asphaltene precipitation is reversible but is likely very slow. The current study suggests that asphaltene precipitation is generally reversible but that the kinetics of the redissolution vary significantly depending upon the physical state of the system.[21]

The variations of the thermodynamic functions in the transitiometric system are determined through their derivatives against one of the (p, V, or T) variables while maintaining other (independent) variables constant.

dx.doi.org/10.1021/ef301449e | Energy Fuels 2013, 27, 1212−1222

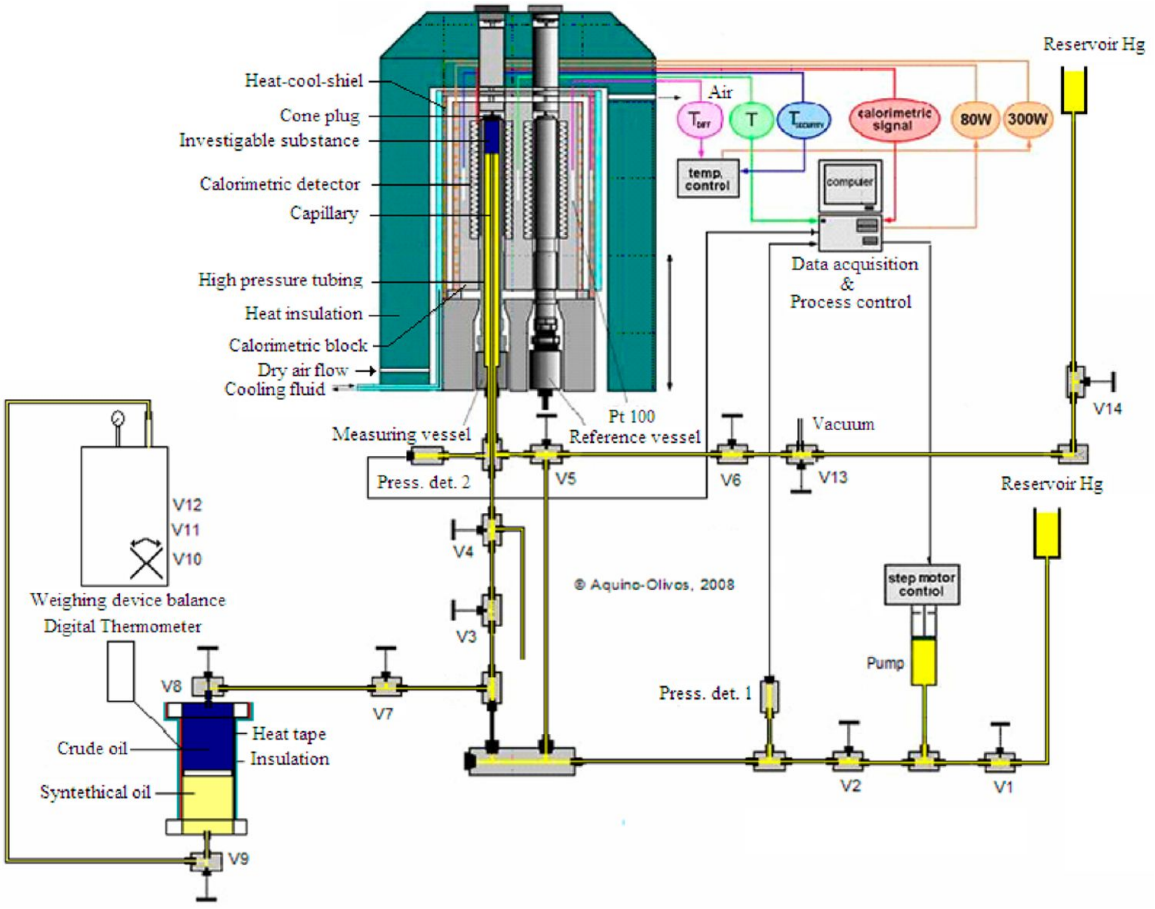

Figure 1. Schematic diagram of the transitiometer used in the determination of the phase transitions of a crude oil sample.

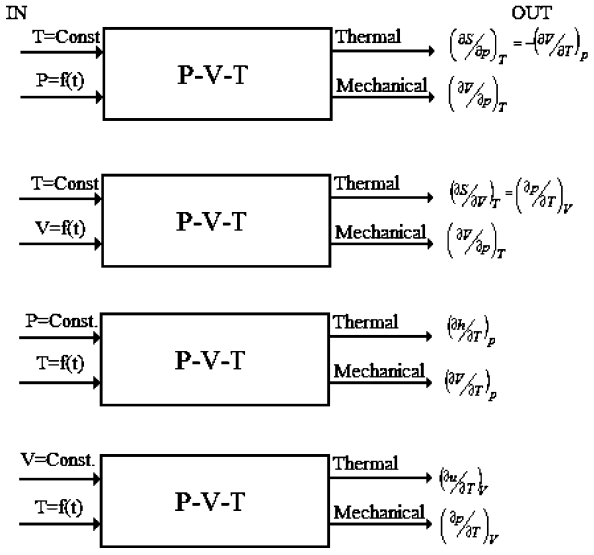

Figure 2. Principle of the scanning transitiometric technique.

In the case where the temperature is constant (isothermal conditions) and the pressure is the inducing variable and is varied as a linear function of time, the scanning transitiometry allows for measurements of $(\partial S/\partial p)_T = -(\partial V/\partial T)_p$ and $(\partial V/\partial p)_T$ simultaneously as thermal and mechanical outputs, respectively.

These thermodynamic derivatives can be determined from the enthalpy function, described by the expression

$$\mathrm{d}h(T, p) = \left(\frac{\partial h}{\partial T}\right)_p \mathrm{d}T + \left(\frac{\partial h}{\partial p}\right)_T \mathrm{d}p \tag{1}$$

and from the change of enthalpy $\mathrm{d}h(T,p)$, expressed as

$$\mathrm{d}h(T, p) = \mathrm{d}Q + V\mathrm{d}p \tag{2}$$

If the temperature is considered to be constant and the pressure is assumed to vary as a linear function of time

$$T = \text{constant}, \quad \mathrm{d}T = 0, \quad p = p_0 + at, \quad \mathrm{d}p = a\mathrm{d}t \tag{3}$$

then eqs 1 and 2 are reduced to the expression

$$\left.\frac{\mathrm{d}Q}{\mathrm{d}t}\right|_T = q_T(p) = \left[\left(\frac{\partial h}{\partial p}\right)_T - V\right]a = \left(\frac{\partial S}{\partial p}\right)_T Ta = -\left(\frac{\partial V}{\partial T}\right)_p Ta \tag{4}$$

where $q_T(p)$ is the heat flow generated or absorbed under isothermal conditions and a is the rate of the linear pressure variation. This is the fundamental thermodynamic principle for pressure-controlled scanning calorimetry (PCSC).[15,22−24]

Crude oil titrations with *n*-heptane were based on the ASTM D3279 and D4124 standard methods. In these ASTM methods, it is mentioned that "... all organic matter that precipitate with *n*-heptane is asphaltene". However, before carrying out these measurements, it was necessary to make some modifications of the original apparatus shown in Figure 1. The new configuration of the system is shown in Figure 3. Figure 1 shows how it is possible to transfer the crude oil sample into the measuring vessel; this configuration being the only way to properly determine asphaltene precipitation onset due to the pressure drop at constant temperature. Figure 3 presents the diagram to perform the

dx.doi.org/10.1021/ef301449e | *Energy Fuels* 2013, 27, 1212−1222

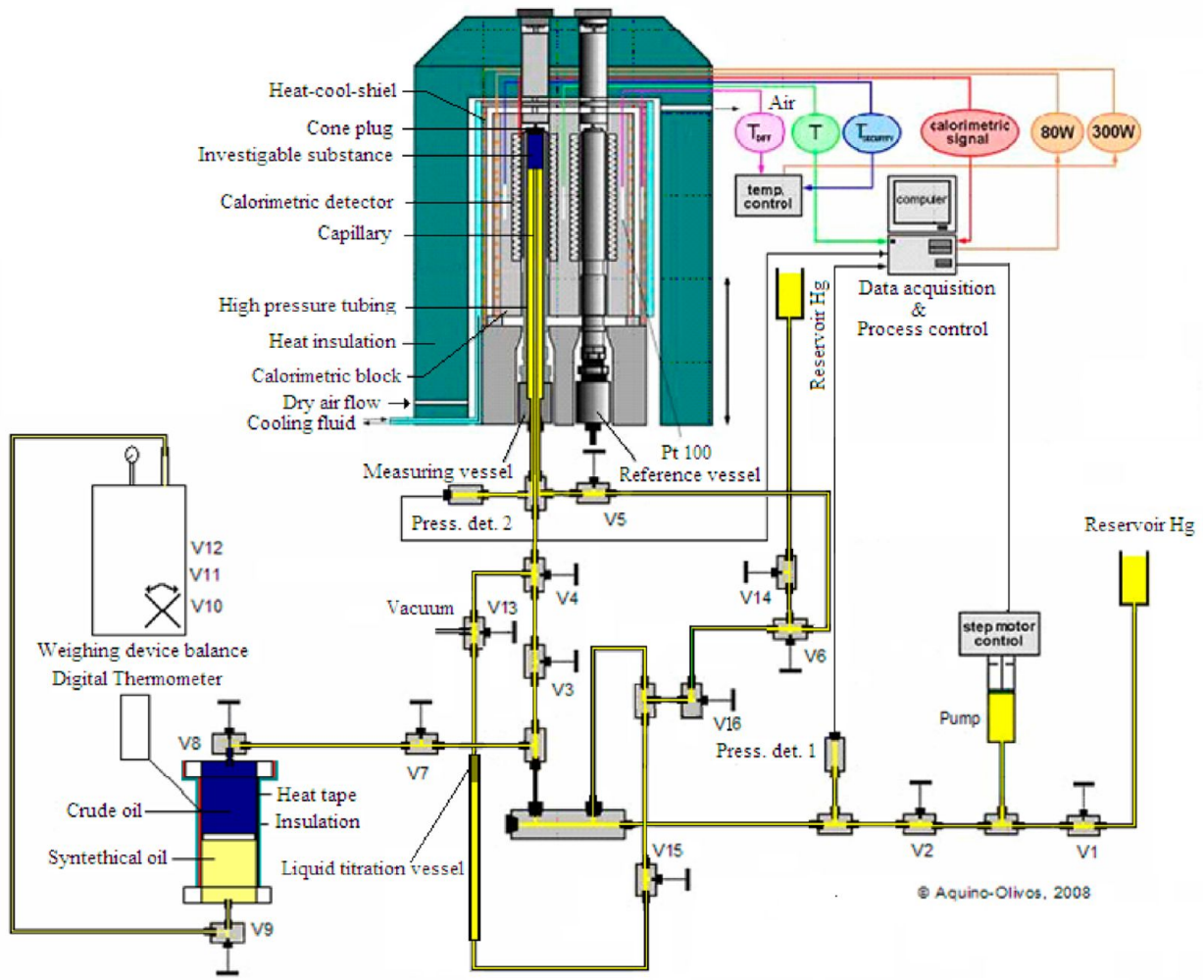

Figure 3. Schematic diagram of the transitiometer used for the titration of a crude oil sample with *n*-heptane.

titration of the crude oil sample with *n*-C_7 at reservoir conditions (at a constant pressure and temperature).[15,16]

In the case of a crude oil titration with *n*-heptane, where the temperature and pressure are constant, it is necessary to introduce the volume as an inducing variable. This can be performed by expressing the differential of the internal energy as

$$du(T, V) = \left(\frac{\partial u}{\partial T}\right)_V dT + \left(\frac{\partial u}{\partial V}\right)_T dV \quad (5)$$

along with the change of internal energy $du(T,V)$, written as

$$du(T, V) = dQ - pdV \quad (6)$$

If the temperature and pressure are constants and the volume is assumed to vary as a linear function of time

$$T = \text{constant}, dT = 0; \qquad p = \text{constant}, dp = 0;$$
$$V = V_0 + ct, dV = cdt \quad (7)$$

then eqs 5 and 6 can be reduced to the expression

$$\left.\frac{dQ}{dt}\right|_T = q_T(V) = \left[\left(\frac{\partial u}{\partial V}\right)_T + p\right]c \quad (8)$$

where $q_T(V)$ is the heat flow generated or absorbed under isothermal conditions and c is the rate of the linear volume variation. Equation 8 allows for calculation of the change in the internal energy when the asphaltene is precipitated with *n*-heptane (or any other titration fluid).

Procedure. A detailed description of the experimental procedure for determining phase transitions, bubble point pressures, and titrations using the transitometric technique is given elsewhere;[15,16] consequently, only the relevant points are briefly presented here. For the determination of the organic matter phase transition and the bubble point pressure, a small amount of the crude oil sample was charged through a concentric capillary.[15,16] In all of the experiments, the volume of the crude oil charged to the vessel was $(2.0 \pm 8.5 \times 10^{-3})$.

Once the crude oil sample was charged into the vessel, the determination of the phase transition and the bubble point pressure was carried out over the pressure range from 5 to 70 MPa. The experiments were carried out under isothermal conditions at four different temperatures: 344, 373, 400, and 427 K. The phase transitions and the bubble point pressure of the crude oil sample were determined at a rate of 2.17×10^{-3} MPa s^{-1}.

On the other hand, the titration of the crude oil sample with *n*-heptane was carried out at 427 K and 30 MPa using the modified transitometric apparatus presented in Figure 3. The crude oil sample phase transition by means of the titration with *n*-heptane was determined at a rate of 1.75×10^{-5} cm^3 s^{-1}. The experiment is based on the ASTM standard methods D3279 and D4124, in which the asphaltene content of petroleum is defined as those components not soluble in *n*-heptane.

RESULTS AND DISCUSSION

Table 1 presents the main properties of the crude oil studied in this work. This table includes the saturates, aromatics, resins, and asphaltenes (SARA) analysis, the gas/oil rate (GOR), and

dx.doi.org/10.1021/ef301449e | Energy Fuels 2013, 27, 1212−1222

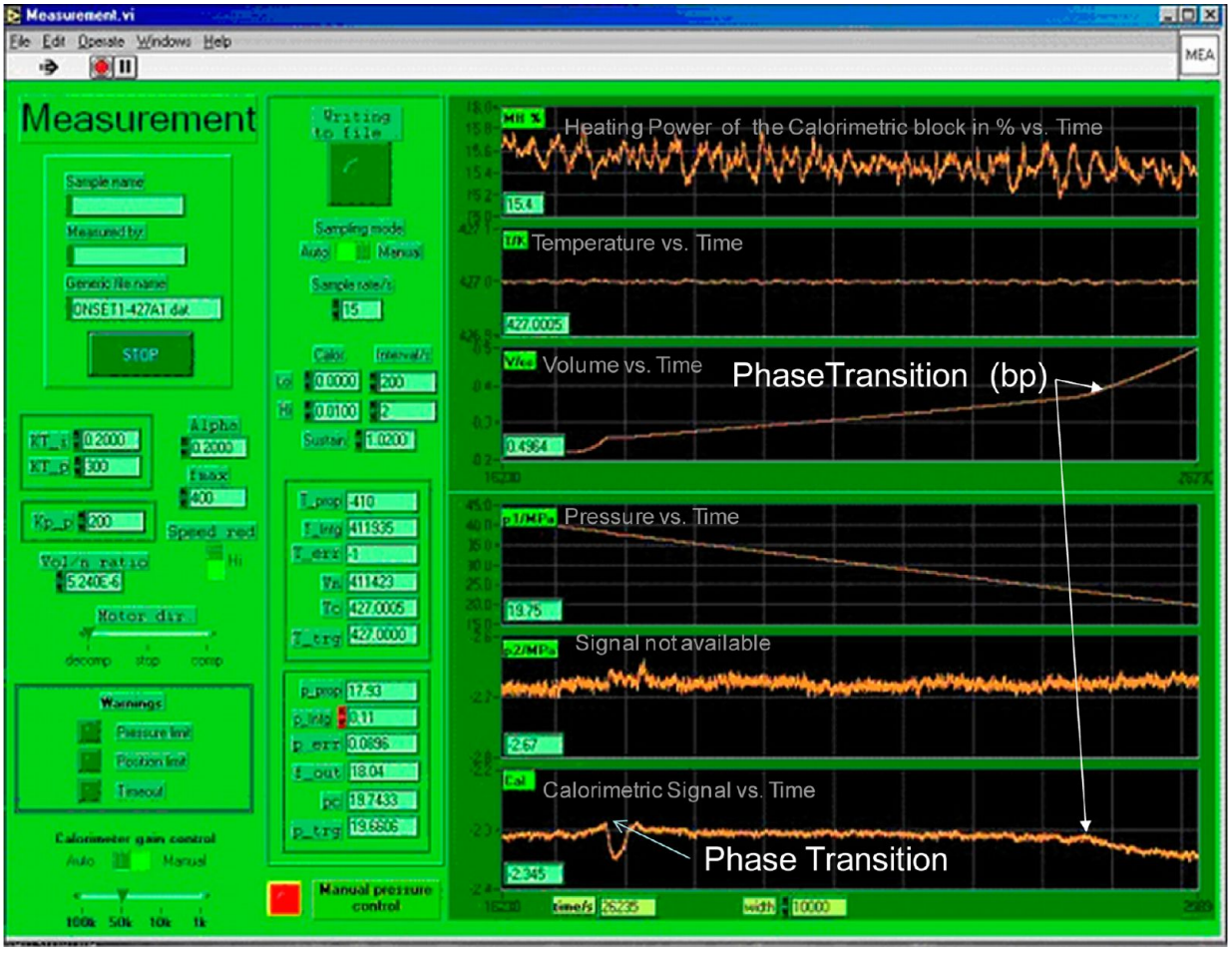

Figure 4. Picture of the measurement parameters for the determination of the phase transitions in a scanning transitiometer.

the density of the oil. In addition, the temperature and pressure of the oil reservoir are also given in this table.

The results on the phase transitions obtained at 427 K are presented in Figure 4. This figure shows, from bottom to top, the gain or loss of the heat power (plot 1), the variation in the pressure of the two pressure transducers (plots 2 and 3), the change in the volume (plot 4), the variation in the temperature (plot 5), and the percent of the heat power variation from the calorimetric block (plot 6). All of these graphs are reported as a function of time. It is important to note in plot 4 that the change of the slope when the gas is liberated from the liquid phase at this point indicates the bubble point pressure of the crude oil. This change in the slope is also observed with a downward peak in plot 1 but in a different direction. Also, it is worth noting a discontinuity (downward peak) in plot 1, which can be attributed to the onset of the organic matter (i.e., asphaltene precipitation).

Figure 5 presents the calorimetric signal as a function of the deceasing pressure at 427 K. In this figure, two phase transitions can be observed: one corresponding to the onset of the asphaltene precipitation at about 39.3 MPa and the other corresponding to the dissolution of the asphaltene at about 9.6 MPa.

Figure 6 shows the variation of the pressure as a function of the volume at 427 K, where a bubble point pressure is observed at about 23.3 MPa, which is determined as the change in the slope when volume increases. This corresponds to a pressure of about 23.3 MPa and a volume of about 0.37 cm^3 in plots of

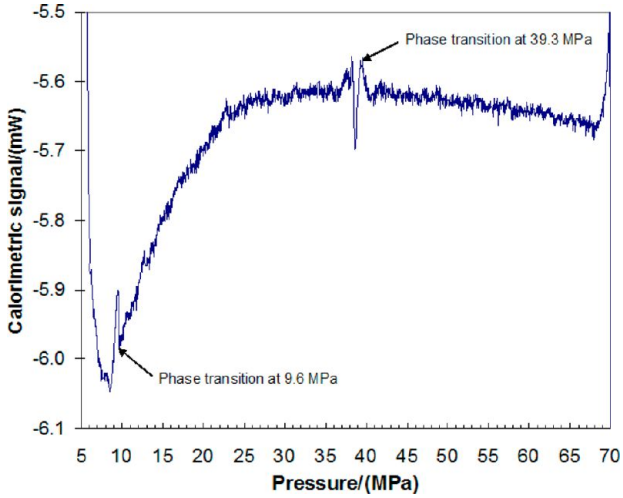

Figure 5. Phase transitions of the organic matter determined at 427 K for the crude oil (A-1) sample.

volume versus time and calorimetric signal versus time, as shown Figure 4, respectively.

Figure 7 shows the compressibility and thermal expansion coefficients $(\partial V/\partial p)_T$ and $(\partial V/\partial T)_p$, respectively, as pressure functions at 427 K. No mathematical methods are necessary to calculate the derivatives; these derivatives are directly obtained by experimental measurements because the two derivatives are

dx.doi.org/10.1021/ef301449e | Energy Fuels 2013, 27, 1212−1222

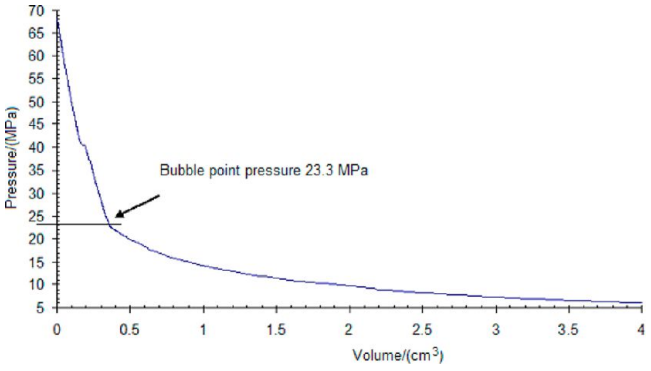

Figure 6. Bubble point pressure determined at 427 K for the crude oil (A-1) sample.

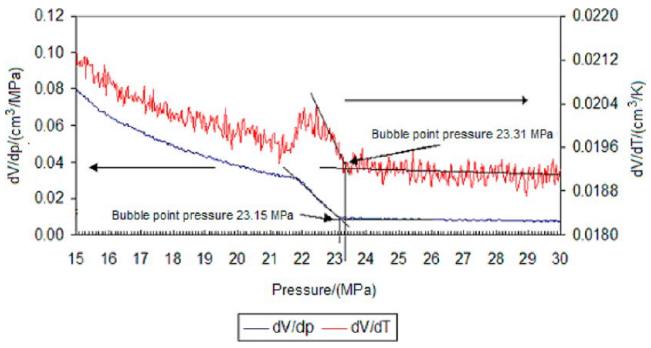

Figure 7. Determination of the crude oil (A-1) bubble point pressure at 427 K by means of the compressibility and thermal expansion coefficients.

obtained from the variations of V versus p or T at constant T or p, respectively. Using the change in the slope for both functions, the resulting bubble point pressures were similar, 23.15 MPa for the first and 23.31 MPa for the second. In both cases, the passage through the phase boundary is clearly observed. These values corroborate the result obtained in Figure 6.

Panels A and B of Figure 8 present the calorimetric signals recorded as functions of the pressure at four different temperatures (344, 373, 400, and 427 K) obtained in this work. These panels show that, at each temperature, two phase transitions occur, similar to those presented in Figure 5, and one bubble point pressure occurs, given in Table 2.

From the phase transitions and bubble point pressures determined at four temperatures investigated over the pressure range from 5 to 70 MPa, the phase diagram of the crude oil sample is constructed using the phase transition and the bubble point pressure results reported in Table 2. Figure 9 presents the phase diagram of the crude oil on the pressure−temperature plane. This figure shows three different curves: one curve corresponding to the onset of the asphaltene precipitation (upper boundary), a second curve corresponding to the line of bubble point pressures, and a third curve corresponding to the asphaltene dissolution (lower boundary). Here, it is worthwhile to mention that the curve of organic matter dissolution is very difficult to obtain using traditional experimental techniques, such as the acoustic technique[25] or the light transmission technique,[26] particularly when aiming to determine the phase transitions and bubble point pressures of heavy crude oils.

To verify that the obtained phase transitions shown in Figure 8 correspond to the asphaltene precipitation and that the lower

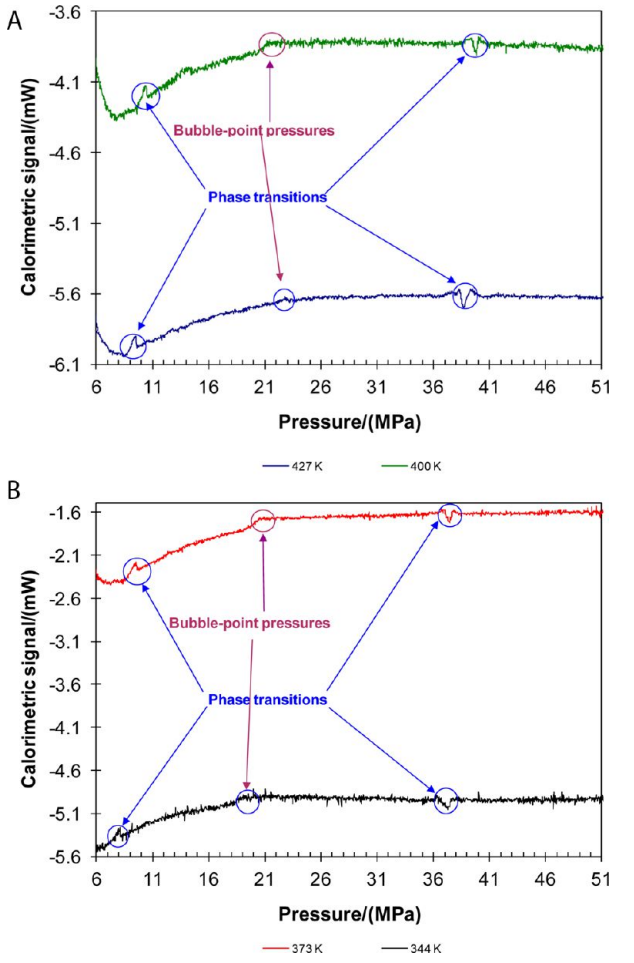

Figure 8. (A and B) Phase transitions of the organic matter and bubble point pressures for the crude oil (A-1) sample.

Table 2. Asphaltene Phase Boundaries and Bubble Point Pressures for the Crude Oil (A-1) Sample

	p (MPa)		
T (K)	lower boundary	upper boundary	bubble point pressure
344.0	8.0	37.5	19.0
373.0	9.7	37.6	20.5
400.0	10.3	39.5	21.5
427.0	10.0	40.0	23.5

and upper boundary curves presented in Figure 9 correspond to the APE of the crude oil, a titration experiment study with *n*-heptane was carried out with the crude oil sample under reservoir conditions. Results obtained of the titration are presented in Figure 10. This figure shows a change on the calorimetric signal at about 7000 s corresponding to the onset of the asphaltene precipitation and the end of the asphaltene precipitation at about 8700 s. The titration time is 1700 s for the phase transition. This indicates that the organic matter envelope shown in Figure 9 corresponds effectively to the APE described above. For this experiment, the asphaltene precipitation is between 12 857 and 13 824 s. The negative volumetric scale in Figure 10 is because, when *n*-C_7 is injected to the system, the pump registers the volume that is displaced to the system and this is negative.

Thermodynamic Modeling. A category of asphaltene precipitation models reported in the literature is that based on

dx.doi.org/10.1021/ef301449e | *Energy Fuels* 2013, 27, 1212−1222

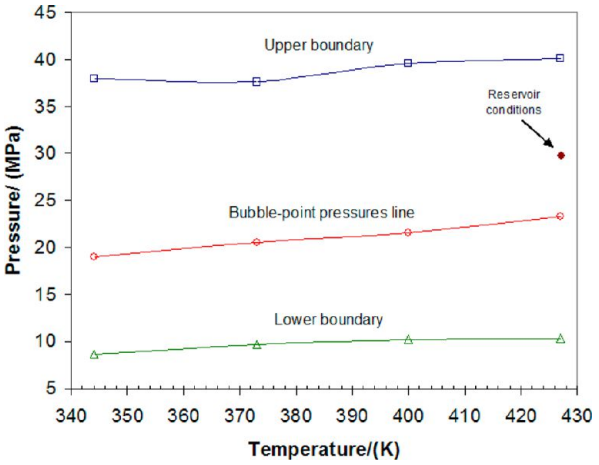

Figure 9. APE for the crude oil (A-1) sample.

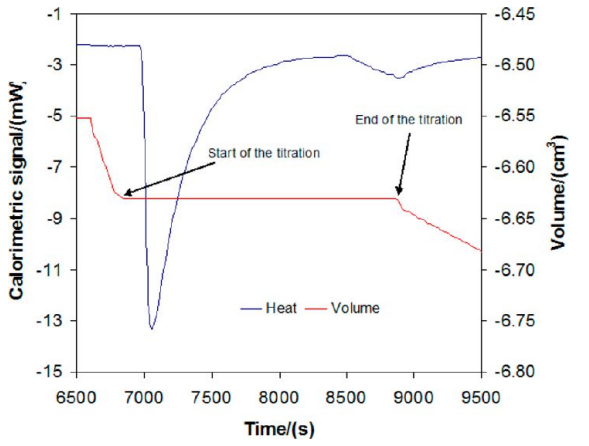

Figure 10. Titration of the crude oil (A-1) sample with *n*-heptane at 427 K and 30 MPa (reservoir conditions of the crude oil).

the description that asphaltene and resin molecules form asphaltene−asphaltene and asphaltene−resin aggregates dispersed in an oil matrix. This description includes the thermodynamic colloidal model,[27] the reversible micellization model,[28,29] and the McMillan−Mayer−SAFT model developed by Wu et al.[30,31] In general, the basic assumption in these models is that a crude oil can be represented by three components: asphaltenes, resins, and solvent. In the thermodynamic colloidal model, asphaltene precipitation is modeled by solving the equilibrium between the absorbed resins into the asphaltenes and resins that are present in the solvent. The micellization model applies the micellization theory proposed by Nagarajan and Ruckenstein,[32] whereas in the McMillan−Mayer−SAFT model, the McMillan−Mayer theory is used to model asphaltenes and resins as solutes in a continuous medium without structure.[33]

Although the asphaltene precipitation phenomenon is a very complex multi-component process that involves a great variety of interactions at molecular and colloidal length scales, Wu et al.[30,31] and Buenrostro-Gonzalez et al.[7] demonstrated that it is possible to theoretically model this system by assuming simplified representations of the crude oil. That is, in solution theories, a basic approximation is to consider the solvent as a structureless continuum with a screening effect over the interactions of solutes, so that the solvent is described by continuous parameters, such as a dielectric constant, refractive index, and density. This approximation was first used by Wu et al. and later by Buenrostro-Gonzalez et al. to develop thermodynamic colloidal models for representing the asphaltene−resin−oil system by considering asphaltenes and resins as solutes dispersed in the oil (i.e., the solvent as a continuous medium without structure).

The thermodynamic colloidal model developed by Buenrostro-Gonzalez et al. was used here for modeling the APE of crude oil A-1. The correlation of the experimental APE data was carried out through the minimization of the differences between experimental pressure data of the upper boundary of the APE and calculated values from the thermodynamic model. A detailed description of the thermodynamic colloidal model to represent the APE of crude oils is given in the paper by Buenrostro-Gonzalez et al., and only the part necessary for the present study will be outlined here.

Description of the Thermodynamic Colloidal Model. The general description of the thermodynamic colloidal model is summarized as follows:[7] (1) asphaltenes and resins are represented by pseudo-pure components, whereas all other oil components are a continuous medium; (2) asphaltene aggregates formed by several molecules are modeled as hard spheres, whereas resin molecules are modeled as hard-sphere chains; (3) interactions between asphaltene and resin molecules are given by potentials of mean force and consist of hard-sphere interactions, van der Waals attraction, and short-ranged anisotropic interactions; (4) the bonding is assumed in a way that asphaltene−asphaltene and asphaltene−resin associations are permitted, but association between resin molecules is not allowed; and (5) asphaltene separation is described as a liquid−liquid equilibrium process.

According to this description, asphaltene and resin molecules consist of single or chained spheres (i.e., monomers) of different diameters that interact by a mean force interaction potential, given by

$$u_{ij}(r) = u_{ij}^{hs}(r_{ij};\ \sigma_{ij}) - \varepsilon_{ij}\phi_{ij}(r_{ij};\ \lambda_{ij}) \tag{9}$$

where $u_{ij}^{hs}(r_{ij};\ \sigma_{ij})$ is the hard-sphere repulsive interaction defined by a diameter σ_{ij} as

$$u_{ij}^{hs}(r_{ij};\ \sigma_{ij}) = \begin{cases} \infty & r_{ij} < \sigma_{ij} \\ 0 & r_{ij} > \sigma_{ij} \end{cases} \tag{10}$$

whereas the attractive interaction has a energy depth $-\varepsilon_{ij}$ and shape $\phi_{ij}(r_{ij};\ \lambda_{ij})$, where λ_{ij} is a parameter related to the range of attractive forces. In eq 9, σ_{ij} and ε_{ij} are the length and energy parameters, respectively, and λ_{ij} is the attractive potential range.

The square well (SW) model is used to describe the shape of the attractive potential ϕ_{ij}

$$\phi_{ij}^{SW}(r_{ij};\ \lambda_{ij}) = \begin{cases} 1 & \text{if} \quad \sigma_{ij} < r_{ij} < \lambda_{ij}\sigma_{ij} \\ 0 & \text{if} \quad r_{ij} > \lambda_{ij}\sigma_{ij} \end{cases} \tag{11}$$

whereas the energy ε_{ij} is estimated from an approximation relating ε_{ij} to the Hamaker constant, which assumes that the medium (i.e., the solvent) affects the phase behavior of an asphaltene-containing crude oil only through the Hamaker constant as

$$\varepsilon_{imj} = \frac{(H_{ii}^{1/2} - H_m^{1/2})(H_{jj}^{1/2} - H_m^{1/2})}{\pi^2 \rho_i^0 \rho_j^0} \tag{12}$$

dx.doi.org/10.1021/ef301449e | *Energy Fuels* 2013, 27, 1212−1222

where ρ_i^0 and ρ_j^0 correspond to the number density of a pure component of the i and j species in terms of the spherical segments, H_{ii} and H_{jj} are the Hamaker constants of the i and j species, and H_m is the Hamaker constant of the medium m, which depends upon its properties. In eq 12, ε_{ij}, which corresponds to its value in vacuum, is replaced by its value in the presence of a solvent (ε_{ijm}) to consider the screen effects caused by the continuous medium m.

The SAFT-VR EoS,[34] used to represent the phases in equilibrium, is given in its general form by

$$\frac{A}{NkT} = \frac{A^{\text{ideal}}}{NkT} + \frac{A^{\text{mono}}}{NkT} + \frac{A^{\text{chain}}}{NkT} + \frac{A^{\text{assoc}}}{NkT} \tag{13}$$

where A is the Helmholtz energy for an oil of N molecules at temperature T, k is the Boltzmann constant, and A^{ideal}, A^{mono}, A^{chain}, and A^{assoc} are the ideal gas, monomer, chain formation, and association contributions to the Helmholtz energy, respectively. In the SAFT-VR EoS, improved expressions to represent the contributions to the Helmholtz energy ascribed to dispersion and associating interactions are considered. The reader is referred to the original paper published by Gil-Villegas et al.[34] for a detailed description of this EoS.

Thus, the parameters of the asphaltene precipitation thermodynamic model are monomer diameters σ_a and σ_r, number of segments (monomers) in the chain m_a and m_r, range of attractive potentials λ_{aa} and λ_{rr}, Hamaker constants H_a and H_r, association energies ψ_{aa} and ψ_{ar}, and number of association sites s_a and s_r, for asphaltene and resin, respectively. In addition, the bonding volume κ, cross-parameters σ_{ar} and λ_{ar}, and the Hamaker constant of the medium H_m are required by the model.

However, the final number of parameters that need to be fitted from experimental data for a particular oil is 7, namely, Hamaker constants H_a and H_r, association energies ψ_{aa} and ψ_{ar}, range of attractive potentials λ_{aa} and λ_{rr}, and the number of association sites s_a for asphaltene. In this case, because the fluid under study is similar in their properties to those fluids reported by Buenrostro-Gonzalez et al.,[7] then three of these parameters used by us and presented in Table 5 are those given by these authors, i.e., Hamaker constants H_a and H_r and the number of association sites s_a for asphaltene. The parameters corresponding to the range of attractive potentials, λ_{aa} and λ_{rr}, were adjusted from the n-C_7 titration of the oil under study for the square-well potential. The remaining two parameter energies, i.e., the association energies ψ_{aa} and ψ_{ar}, were fitted from two experimental points of the APE. In our case, the two experimental points used in the adjustment of these parameters are indicated in Table 6.

According to Buenrostro-Gonzalez et al., although the number of molecular parameters of the model seems to be rather high, several of these parameters have a physical meaning based on colloidal and molecular models used to represent asphaltenes, resins, and the interactions among them. This means that most of the model parameters can be obtained by experimental procedures, fixed by model assumptions, or calculated through specific relationships or theoretical results. Consequently, as mentioned above, only seven parameters (H_a, H_r, λ_{aa}, λ_{rr}, ψ_{aa}, ψ_{ar}, and s_a) need to be determined from experimental data for a particular oil.

Because the asphaltene precipitation is considered as a liquid−liquid separation, then the conditions for liquid−liquid isothermal equilibrium are given by the equality of the chemical potentials for asphaltene, $\mu_a = (\partial A/\partial N_a)_{T,V,N_r}$, and resin, $\mu_r = (\partial A/\partial N_r)_{T,V,N_a}$, and the equality of the osmotic pressures π in the equilibrated phases $'$ and $''$ (with the higher density liquid phase being the precipitated phase), i.e.,

$$\mu'_a = \mu''_a \tag{14}$$

$$\mu'_r = \mu''_r \tag{15}$$

$$\pi' = \pi'' \tag{16}$$

The osmotic pressure π is obtained from the thermodynamic relationship

$$\frac{\pi V}{NkT} = \hat{x}_a \frac{\mu_a}{kT} + \hat{x}_r \frac{\mu_r}{kT} - \frac{A}{NkT} \tag{17}$$

where V is the total volume of the phase, A is the Helmholtz energy, and $\hat{x}_i$ ($i = a, r$) is the effective molar fraction of a pseudo-binary mixture, which only depends upon the solute properties.

The onset of the asphaltene precipitation pressure is obtained through the Gibbs energy surface analysis by minimizing the tangent plane distance, expressed as[35]

$$\text{TPD}(\boldsymbol{x}) = \sum_{i=i}^{n=a,r,m} x_i[\mu_i(\boldsymbol{x}) - \mu_i(\boldsymbol{z})] \tag{18}$$

where the chemical potential μ_i is evaluated at the trial phase composition $\boldsymbol{x}$ and the overall composition of the mixture $\boldsymbol{z}$ for a given pressure and temperature. In eq 18, the medium is also considered for the phase stability analysis together with asphaltene and resin. Asphaltene precipitation occurs when $\text{TPD}(\boldsymbol{x}) < 0$, and the pressure at which this happens corresponds to the onset of the asphaltene precipitation pressure. The amount of asphaltene precipitated is calculated by solving the liquid−liquid equilibrium conditions in terms of the chemical potential μ_i ($i = a, r$) and the osmotic pressure π in conjunction with the equations given by the mass balance restrictions, as described by Buenrostro-Gonzalez et al. In this case, the values of composition $\boldsymbol{x}$ provided by phase-stability analysis are used as the initial guesses.

Calculation of the APE for Crude Oil A-1. To model the asphaltene precipitation for a reservoir fluid at given pressure and temperature conditions, it is necessary to perform first a vapor−liquid equilibrium calculation using an EoS to obtain the composition and fluid properties of the liquid phase at equilibrium. Then, using the model system asphaltene−resin−oil, a stability analysis is applied to find the pressure corresponding to the initial (onset) asphaltene precipitation. Finally, the amount of asphaltene precipitated is calculated by solving the liquid−liquid equilibrium equations described previously.

Table 3 presents the data obtained from the characterization of crude oil A-1, which was taken directly from the bottom of the well and was preserved by maintaining its sampling pressure until the moment of being used in the experiments. For this live oil, the C_{7+} fraction ($x_{C_{7+}} = 0.235$) was divided into six pseudo-components based on known average molecular weight, average density, and an assumed variance. The γ distribution function was used to represent the C_{7+} fraction, and the molecular weight and molar fraction for the six pseudo-components were determined using the Gaussian quadrature method, as presented by Cotterman et al.[36,37] Twu's correlations[38] were used to calculate the critical properties of the six pseudo-

dx.doi.org/10.1021/ef301449e | Energy Fuels 2013, 27, 1212−1222

Table 3. Characterization Data for Crude Oil A-1[a]

component	mol fraction	pseudo-component	mol fraction
CO_2	0.0197	$C_{7+(1)}$	0.0025
H_2S	0.0074	$C_{7+(2)}$	0.0441
N_2	0.0101	$C_{7+(3)}$	0.1142
methane	0.3939	$C_{7+(4)}$	0.0659
ethane	0.1304	$C_{7+(5)}$	0.0082
propane	0.0917	$C_{7+(6)}$	0.0001
isobutane	0.0157		
n-butane	0.0392		
isopentane	0.0180		
n-pentane	0.0162		
C_6	0.0267		

[a]Reservoir conditions: T = 427 K and p = 29.73 MPa.

components, whereas the Lee−Keesler correlation[39] was used to estimate the acentric factors.

The vapor−liquid equilibrium calculation for the oil A-1 was performed using the PR (Peng−Robinson) EoS[40] with translation in the volume[41] to determine the density and composition of the liquid phase. The binary interaction parameters k_{ij} used for interactions among the dissolved gases (N_2, CO_2, and H_2S) and hydrocarbons were taken from Katz and Firoozabadi,[42] whereas the binary interaction parameters among the hydrocarbon components were calculated using the formula by Chueh and Prausnitz[43]

$$k_{ij} = 1 - \left(\frac{2V_{c,i}^{1/6} V_{c,j}^{1/6}}{V_{c,i}^{1/3} + V_{c,j}^{1/3}} \right)^{\theta} \tag{19}$$

where $V_{c,i}$ is the critical volume of component i and θ is an adjustable parameter, which is obtained from the regression of the bubble point pressure data. Here, a value of θ = 0.906 was obtained from the correlation of the experimental bubble point pressure data determined at four temperatures for oil A-1 (see Table 4) by minimizing the following objective function:

$$F_{bp} = \sum_{i=1}^{4} \left(\frac{p_{bp,i}^{expl} - p_{bp,i}^{calc}}{p_{bp,i}^{expl}} \right)^2 \tag{20}$$

Table 4. Experimental and Calculated Bubble Point Pressures for Crude Oil A-1

	p (MPa)		
T (K)	experimental	calculated	percent error (%)[a]
427.0	23.3	22.7	−2.6
400.0	21.5	21.8	1.5
373.0	20.5	20.5	0.2
344.0	19.0	18.6	−1.9

[a]Percent error = 100 × $(1 - p_{bp}^{calc}/p_{bp}^{expl})$.

where $p_{bp,i}^{expl}$ and $p_{bp,i}^{calc}$ are the experimental and calculated bubble pressures for an experiment i, respectively.

Table 4 presents the experimental and calculated bubble pressures for oil A-1. As seen in this table, the maximum error obtained from the regression (2.6%) corresponds to the calculated bubble pressure at 427 K (see Figure 11), indicating that the PR EoS could sub-predict the bubble pressure line of the phase envelope for this oil at higher temperatures.

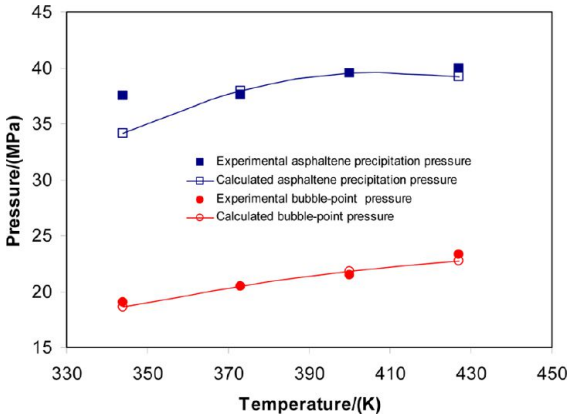

Figure 11. Experimental and calculated phase diagram of the APE and bubble point pressure line for crude oil A-1.

The molecular parameters used in this work for modeling the asphaltene phase envelope of crude oil A-1 are given in Table 5.

Table 5. Parameters of the Thermodynamic Colloidal Model for Crude Oil A-1

s_a	H_a/k^a (K)	H_r/k^a (K)	λ_{aa} (K)	λ_{rr} (K)	ψ_{aa}/k^a	ψ_{ar}/k^a
2	11270.01[b]	1891.03[b]	4.198	4.540	2826.71	3274.47

[a]k = 1.381 × 10^{-23} J K^{-1} (Boltzmann constant) [b]From ref 26.

The remaining parameters of the model are those reported by Buenrostro-Gonzalez et al.;[7] i.e., σ_a = 1.7 nm, σ_r = 0.5 nm, m_a = 1, m_r = 10, κ = 0.5, and s_r = 1. The cross-parameters of the mixture σ_{ar} and λ_{ar} are calculated through the following combining rules:[44]

$$\sigma_{ar} = \frac{\sigma_a + \sigma_r}{2} \tag{21}$$

$$\lambda_{ar} = \frac{\lambda_a \sigma_a + \lambda_r \sigma_r}{\sigma_a + \sigma_r} \tag{22}$$

whereas the Hamaker constant of the medium m, H_m, is estimated from a pairwise additivity approximation, given by

$$H_m = \sum_i \sum_j \pi^2 B_{ij} \rho_i \rho_j \tag{23}$$

where $B_{ij} = (B_i B_j)^{1/2}$ is the cross-London dispersion constant for groups i and j (i and j refer to CH_4, N_2, CO_2, H_2S, and CH_2 groups) and ρ_i is the number density for each component in the liquid phase at given temperature and pressure conditions. Equation 23 is the contribution of light components to the Hamaker constant of the medium. It is used because the calculation of asphaltene precipitation in a live-oil sample involves the estimation of the medium properties H_m and ρ_m, considering the light components dissolved in oil at given values of pressure and temperature.

Parameters ψ_{aa} and ψ_{ar} were calculated using two experimental asphaltene precipitation pressures of the APE through the minimization of the following objective function:

$$F_{onset} = \sum_{i=1}^{2} \left(\frac{p_{onset,i}^{expl} - p_{onset,i}^{calc}}{p_{onset,i}^{expl}} \right)^2 \tag{24}$$

dx.doi.org/10.1021/ef301449e | Energy Fuels 2013, 27, 1212−1222

where p_{onset}^{expl} and p_{onset}^{calc} are the experimental and calculated pressures at the beginning of the asphaltene precipitation, respectively.

Table 6 presents the experimental asphaltene precipitation pressures of APE for oil A-1 as well as the results of the regression using the thermodynamic colloidal model along with the SAFT-VR EoS. As seen in this table, the agreement between the experimental and calculated asphaltene precipitation onsets is good for the two chosen temperatures (373 and 400 K). When the asphaltene precipitation onset is predicted at 427 K (the highest temperature of the study), the agreement is still satisfactory; however, at 344 K, the prediction is rather poor (8.8%).

Table 6. Experimental and Calculated Asphaltene Precipitation (Onset) Pressures for Oil A-1

	p (MPa)		
T (K)	experimental	calculated	percent error (%)[a]
427.0	40.0	39.2	2.0
400.0[a]	39.5[b]	39.5	0.0
373.0[a]	37.6[b]	37.9	−0.8
344.0	37.5	34.2	8.8

[a]Percent error = $100 \times (1 - p_{onset}^{calc}/p_{onset}^{expl})$. [b]Data used to determine ψ_{aa} and ψ_{ar}.

Figure 11 shows, on a pressure−temperature phase diagram, the experimental and calculated asphaltene precipitation pressures of the upper boundary of the APE for oil A-1. This figure shows the capability of the thermodynamic colloidal model to represent and predict the measured asphaltene precipitation onsets for this oil. An inspection of this figure indicates that the predicted points at 344 and 427 K are rather sub-predicted, although this effect is more pronounced at the lowest temperature of study. This figure clearly shows that it is necessary to include all of the experimental asphaltene precipitation pressures to adjust parameters ψ_{aa} and ψ_{ar} to give a more satisfactory representation of the APE for this oil. However, the idea of using only two experimental data in the regression was to test the predictive capability of the thermodynamic colloidal model used here.

Figure 11 also shows the experimental and calculated bubble point pressures using the PR EoS. Overall, it can be said that the performance of this EoS to represent the bubble pressure line is, in general, satisfactory.

Finally, the procedure presented above to calculate the amount of precipitated material (asphaltenes and resins) as a liquid−liquid separation was applied. In this case, the amount of precipitated asphaltenes and resins for oil A-1 was 0.5 and 6.0 mass %, respectively. A direct comparison of these calculated values of precipitated material was not possible because there are not experimental data. An experimental methodology to determine the rates of precipitated material for live oils is presently in progress.

CONCLUSION

In this work, a novel method of determination of both phase transitions and bubble point pressures of crude oils has been applied successfully for a Mexican crude oil sample. Phase transitions determined in this method were the onset and dissolution points of the organic matter precipitated at four different temperatures by scanning pressure. A titration test with *n*-heptane was also applied at reservoir conditions for the crude oil sample realizing the determination of the calorimetric signal, verifying the onset of the asphaltene where the precipitation starts. This titration experiment also corroborates that the organic matter envelope corresponds to the APE.

The advantage of the transitiometric technique is the small quantity of fluid under study for the determination of the whole envelope of the organic matter. Moreover, this technique can also be used to determine the phase transitions and the bubble point pressures for other crude oils, such as heavy and extra-heavy types, because of its principle of measurement based on the sensitive calorimetric signal.

A thermodynamic colloidal model reported in the literature was used to correlate and predict the upper boundary of the APE for a Mexican live oil (crude oil A-1). Two experimental asphaltene precipitation pressures were used to adjust the two association energies existing in the association contribution of the Helmholtz energy according in the SAFT-VR approach. Results of the correlation showed that the model was able to represent successfully the two experimental data used for this purpose. However, predictions at other temperatures are less satisfactory, particularly at lower temperatures. Hence, it is more convenient to include all of the experimental pressures at the onset of precipitation to obtain a correct representation of the APE.

The bubble point pressure line of the phase envelope for oil A-1 was satisfactorily represented with the PR EoS using an adjustable parameter to calculate the binary interaction parameters among hydrocarbons and recommended binary interaction parameters to account for the interactions among the dissolved gases (N_2, CO_2, and H_2S) and hydrocarbons.

AUTHOR INFORMATION

Corresponding Author

*Telephone: +52-55-9175-8118. Fax: +52-9175-6426. E-mail: maquino@imp.mx.

Notes

The authors declare no competing financial interest.

ACKNOWLEDGMENTS

Marco A. Aquino-Olivos gratefully acknowledges the Mexican Petroleum Institute for their scholarship support to carry out this work at the Laboratoire de Thermodynamique des Solutions et des Polymères at Université Blaise-Pascal of Clermont-Ferrand, France. The authors thanks Dr. Eduardo Buenrostro-González for providing a copy of the computer code to perform the asphaltene precipitation modeling for oil A-1.

REFERENCES

(1) Joshi, N. B.; Mullins, O. C.; Jamaluddin, A.; Creek, J.; McFadden, J. *Energy Fuels* **2001**, *15*, 979−986.
(2) Vazquez, D.; Mansoori, G. A. *J. Pet. Sci. Eng.* **2000**, *26*, 49−55.
(3) Bucaram, S. M. *J. Pet. Technol.* **1967**, *19*, 150−162.
(4) Karan, K.; Hammami, A.; Flannery, M.; Stankiewicz, B. A. *Pet. Sci. Technol.* **2003**, *21*, 629−645.
(5) http://www.spe.org/glossary/wiki/doku.php/terms:deferred_production.
(6) Stachowiak, Ch.; Grolier, J.-P. E.; Randzio, S. L. *Energy Fuels* **2001**, *15*, 1033−1037.
(7) Buenrostro-González, E.; Lira-Galeana, C.; Gil-Villegas, A.; Wu, J. *AIChE J.* **2004**, *50*, 2552−2570.
(8) Randzio, S. L. *Chem. Soc. Rev.* **1996**, *25*, 383−392.
(9) Randzio, S. L.; Grolier, J.-P. E. *Anal. Chem.* **1998**, *70*, 2327−2330.

(10) Wilken, M.; Fisher, K.; Gmehling, J. *Chem. Eng. Technol.* **2002**, *25*, 779−784.
(11) Randzio, S. L.; Stachowiak, Ch.; Grolier, J.-P. E. *J. Chem. Thermodyn.* **2003**, *35*, 639−648.
(12) Randzio, S. L. *J. Therm. Anal. Calorim.* **2007**, *89*, 52−59.
(13) Aquino-Olivos, M. A.; Grolier, J.-P. E.; Randzio, S. L.; Aguirre-Gutiérrez, A. J.; García-Sánchez, F. *J. Chem. Eng. Data* **2010**, *55*, 5497−5503.
(14) Randzio, S. L.; Stachowiak, Ch.; Grolier, J.-P. E. *J. Chem. Thermodyn.* **2003**, *35*, 639−648.
(15) Aquino-Olivos, M. A. Transitometric determination of asphaltenes precipitation envelopes at reservoir conditions (in Spanish). Doctoral Thesis, Instituto Mexicano del Petróleo, México, D.F., México, 2010.
(16) Aquino-Olivos, M. A.; Grolier, J.-P. E.; Randzio, S. L. Méthode de transfert sous pression d'un fluide issu d'un gisement de ce fluide et dispositif de mise en oeuvre d'une telle méthode. Patent, reference BFF 11A0945/GB.
(17) Pfieffeer, J. P.; Saal, R. N. J. *J. Phy. Chem.* **1940**, *44*, 139−149.
(18) Fotland, P. *Fuel Sci. Technol. Int.* **1996**, *14*, 313−325.
(19) Wang, J. X.; Brower, K. R.; Buckley, J. S. *Proceedings of the Society of Petroleum Engineers (SPE) International Symposium on Oilfield Chemistry*; Houston, TX, 1999; SPE 50745, pp 16−19.
(20) Hirschberg, A.; de Jong, L. N.; Schipper, B. A.; Meijer, J. G. *SPE J.* **1984**, *24*, 283−293.
(21) Hammami, A.; Phelps, C. H.; Monger-McClure, T.; Little, T. M. *Energy Fuels* **2000**, *14*, 14−18.
(22) Randzio, S. L. *J. Phys. E: Sci. Instrum.* **1983**, *16*, 691−694.
(23) Randzio, S. L. *J. Phys. E: Sci. Instrum.* **1984**, *17*, 1058−1061.
(24) Randzio, S. L.; Grolier, J.-P. E.; Quint, J. R. *Rev. Sci. Instrum.* **1994**, *65*, 960−965.
(25) Sivaraman, A.; Hu, Y.; Jamaluddin, A. K. M.; Thomas, F. B.; Bennion, D. B. Asphaltene onset, effects of inhibitors and EOS modeling of solids precipitation in live oil using acoustic resonance technology. *Proceedings of the American Institute of Chemical Engineers (AIChE) Spring National Meeting*; Houston, TX, 1999; pp 14−18.
(26) Aquino-Olivos, M. A.; Andersen, S. I.; Lira-Galeana, C. *Pet. Sci. Technol.* **2003**, *21*, 1017−1041.
(27) Leontaritis, K. J.; Mansoori, G. A. Asphaltene flocculation during oil production and processing: A thermodynamic colloidal model. *Proceedings of the Society of Petroleum Engineers (SPE) International Symposium on Oil Field Chemistry*; San Antonio, TX, 1987; SPE 16258, pp 4−6.
(28) Victorov, A. I.; Firoozabadi, A. *AIChE J.* **1996**, *42*, 1753−1764.
(29) Pan, H. K.; Firoozabadi, A. Thermodynamic micellization model for asphaltene precipitation from reservoir crude at high pressures and temperatures. *Proceedings of the Society of Petroleum Engineers (SPE) Annual Technical Conference and Exhibition*; San Antonio, TX, 1997; SPE 38857, pp 5−8.
(30) Wu, J.; Prausnitz, J. M.; Firoozabadi, A. *AIChE J.* **1998**, *44*, 1188−1199.
(31) Wu, J.; Prausnitz, J. M.; Firoozabadi, A. *AIChE J.* **2000**, *46*, 197−209.
(32) Nagarajan, R.; Ruckenstein, E. *Langmuir* **1991**, *7*, 2934−2969.
(33) Prausnitz, J. M.; Lichtenthaler, R. N.; Gomes de Acevedo, E. *Molecular Thermodynamics of Fluid Phase Equilibria*, 3rd ed.; Prentice-Hall PRT: Upper Saddle River, NJ, 1999.
(34) Gil-Villegas, A.; Galindo, A.; Whitehead, P. J.; Mills, S.; Jackson, G. J. *Chem. Phys.* **1997**, *106*, 4168−4186.
(35) Baker, L. E.; Pierce, A. C.; Luks, K. D. *Soc. Pet. Eng.* **1982**, *22*, 731−742.
(36) Cotterman, R. L.; Prausnitz, J. M. *Ind. Eng. Chem. Process Des. Dev.* **1985**, *24*, 434−443.
(37) Cotterman, R. L.; Chou, G. F.; Prausnitz, J. M. *Ind. Eng. Chem. Process Des. Dev.* **1986**, *25*, 840−841.
(38) Twu, C. H. *Fluid Phase Equilib.* **1984**, *16*, 137−150.
(39) Reid, R. C.; Prausnitz, J. M.; Poling, B. E. *The Properties of Gases and Liquids*, 4th ed.; McGraw-Hill: New York, 1987.
(40) Peng, D. Y.; Robinson, D. B. *Ind. Eng. Chem. Fundam.* **1976**, *15*, 59−64.
(41) Peneloux, A.; Rauzi, E.; Freze, R. *Fluid Phase Equilib.* **1982**, *8*, 7−23.
(42) Katz, D. L.; Firoozabadi, A. *J. Pet. Technol.* **1978**, *Nov.*, 1649−1655.
(43) Chueh, P. L.; Prausnitz, J. M. *AIChE J.* **1967**, *13*, 1099−1107.
(44) Galindo, A.; Davis, L. A.; Gil-Villegas, A.; Jackson, G. *Mol. Phys.* **1998**, *93*, 241−252.